551·558·21

A theoretical study of Mountain Waves on Western Ghats

R. P. SARKER

Institute of Tropical Meteorology, Poona

(Received 19 February 1965)

ABSTRACT. The paper presents the results of a theoretical investigation on the occurrence of mountain waves on the lee of Western Ghats. The average E-W vertical cross-section of the ghats is represented by a mathematical expression and the expressions for vertical velocity and displacement of streamlines are established for a two-dimensional motion making appropriate approximation in the lee-wave equation. Computation has been made for six cases for the winter season when the wind is more or less westerly and the atmosphere is dry. It appears wave lengths less than 25 km are not important for the Western Ghats. It is only the longer waves that give appreciable amplitudes. The various cases are discussed in terms of the distribution of wind speed and stability.

1. Introduction

The mountain wave phenomenon or better known as the lee wave associated with a mountain has been the subject of theoretical investigations by many workers. The classical investigations in this field are due to Rayleigh (1883) and Kelvin (1886) who studied waves in a stream of water set up by an obstacle on the bed or near surface. Lyra (1943) and Queney (1947) studied waves in the stratified atmosphere and gave solutions for air stream having uniform velocity and stability. It was Scorer (1949, 1953) who first introduced the variation of stability and wind speed with height. His simplified perturbation equation is —

$$\frac{\partial^2 \psi}{\partial z^2} + (l^2 - k^2)\,\psi = 0 \qquad (1)$$

where ψ is the stream function of the disturbance, and

$$l^2 = \frac{g\beta}{U^2} - \frac{1}{U} \cdot \frac{d^2U}{dz^2} \qquad (2)$$

β is the stability parameter $(1/\theta)\,(d\theta/dz)$, θ the potential temperature, U the undisturbed wind speed assumed to be a function of z only and g, the acceleration due to gravity. k is the wave member.

Scorer showed from equation (1) that no lee wave can occur with l^2=constant. This notion led Scorer to introduce the concept of interface in the air stream dividing it into two or three layers in each of which l^2 has a constant but different value and he found that in order that lee wave should occur, l^2 must decrease upwards.

Sawyer (1960) studied the numerical solution of the wave equation (1) with the aid of an electronic computer which enabled him to take various forms of l^2.

Palm (1958), Palm and Foldvik (1960), Foldvik and Palm (1957, 1959) were the first to represent the l^2 profile by an analytical function of the form

$$f(z) = f_0 \cdot e^{-\lambda z}$$

A similar method was also adopted by Döös (1958, 1961, 1962) independently. However, while Döös approximated the l^2-profile by a single exponential function for the entire atmosphere, Palm and Foldvik divided the atmosphere into 2 or 3 layers and replaced l^2 in each layer by a different appropriate expression, constant or exponential. It must, however, be recognised that the main emphasis by Palm and Foldvik was given to longer waves which necessitated them to take mean wind and stability at higher levels than that recorded by sounding balloons. It was again shown by Palm and Foldvik (1960) as well as by Corby and Sawyer (1958) and Sawyer (1960) that the motion in the lower troposphere (5 to 6 km) is independent of the behaviour of $f(z)$ above the level where $f(z)$ attains its minimum value. The real

distribution of $f(z)$ in the stratosphere may, therefore, be represented by an artificial distribution for simplification. Accordingly, Palm and Foldvik (1960) approximated the observed values of $f(z)$ by an exponential function and considering the motion in the lower troposphere this function was chosen to represent $f(z)$ in the entire atmosphere. Foldvik (1962) applied it further for rapid calculation of wavelength and vertical velocity for a symmetrical mountain profile.

A similar method has been applied in the present paper for the investigation of mountain waves in the Western Ghats.

2. The lee-wave equation

We consider the two-dimensional motion in the vertical plane with z-axis vertical and the x-axis directed along the undisturbed current U which is assumed to be a function of height only. The air stream blows perpendicularly to the mountain ridge which is considered to have an infinite extent along the N-S direction.

We assume (*i*) that the undisturbed quantities are functions of z only; (*ii*) that the perturbation quantities are small so that their product and higher order terms may be neglected compared to the undisturbed quantities; (*iii*) that the motion is non-viscous and laminar. Condensation and earth's rotation are neglected.

How far the neglect of earth's rotation is justified can be seen from the following consideration. If u is the perturbation velocity, the acceleration due to coriolis effect is fu, f being the coriolis parameter. Acceleration arising from the advective changes in cross-mountain motion is $U(\partial u/\partial x)$, where U is the stream velocity. The advective acceleration is of basic importance in the mountain effect. The coriolis acceleration can be neglected compared to the advective acceleration if

$$f u << U \frac{\partial u}{\partial x}, \text{ i.e., if } f << U \frac{\partial}{\partial x} \sim \frac{2\pi U}{L}$$

where L is the horizontal wavelength. Thus for an Indian latitude and for a stream velocity of $U=10$ m/sec, the coriolis acceleration will be less than 1/10 of the advective acceleration if $L<150$ km. It will be seen later that in all our cases studied, the wavelength is less than this limit which justifies the neglect of coriolis force.

We also assume that the motion is steady.

The basic equations are — two equations of motion, the equation of continuity, the equation of state and the adiabatic equation. Starting with these equations and after linearisation and elimination we get for w, the vertical perturbation velocity, the following differential equation —

$$\left(1 - \frac{U^2}{C^2}\right)\frac{\partial^2 w}{\partial x^2} + \frac{\partial^2 w}{\partial z^2} - \left(\frac{g}{RT} - \frac{\chi R\nu + 2U(dU/dz)}{C^2 - U^2}\right)\frac{\partial w}{\partial z} + \left[\frac{(\chi-1)g^2}{C^2 U^2} - \frac{g\chi R\nu}{(C^2-U^2)U^2} - \frac{1}{U}\frac{d^2U}{dz^2} + \left(\frac{\chi g}{C^2} - \frac{\chi R\nu + 2g}{C^2 - U^2}\right)\frac{1}{U}\frac{dU}{dz} - \frac{2}{C^2-U^2}\left(\frac{dU}{dz}\right)^2\right] w = 0 \qquad (3)$$

where $C^2 = \chi RT$ and $\chi = g/(g - R\nu^*)$

R is the gas constant for unit mass. ν^* is the adiabatic lapse rate, dry or moist. T is the undisturbed temperature, and $\nu = -(dT/dz)$ is the actual lapse rate in the undisturbed atmosphere, g is the acceleration due to gravity.

In equation (3) we can with very good approximation neglect U^2 in comparison to C^2 whether the air is dry or moist.

Equation (3) then reduces to

$$\frac{\partial^2 w}{\partial x^2} + \frac{\partial^2 w}{\partial z^2} - \left(\frac{g - R\nu}{RT} - \frac{2U}{\chi RT} \cdot \frac{dU}{dz} \right) \frac{\partial w}{\partial z} + \left[\frac{g(\nu^* - \nu)}{U^2 T} - \frac{1}{U} \frac{d^2 U}{dz^2} + \left(\frac{\nu^* - \nu}{T} - \frac{g}{\chi RT} \right) \frac{1}{U} \cdot \frac{dU}{dz} - \frac{2}{\chi RT} \left(\frac{dU}{dz} \right)^2 \right] w = 0 \quad (4)$$

Again the second term in the coefficient of $\partial w/\partial z$ can be neglected compared to the first one. For, the lapse rate is always less than 10°C/km, the maximum wind shear in the examples that we shall consider will never exceed 20 kt per km, *i.e.*, 10 m/sec per km and the maximum wind speed will not exceed 100 kt, *i.e.*, 50 m/sec. With these extreme values the ratio of the second to the first term will be less than 1/10, so that equation (4) further reduces to —

$$\frac{\partial^2 w}{\partial x^2} + \frac{\partial^2 w}{\partial z^2} - \frac{g - R\nu}{RT} \cdot \frac{\partial w}{\partial z} + \left[\frac{g(\nu^* - \nu)}{U^2 T} - \frac{1}{U} \frac{d^2 U}{dz^2} + \left(\frac{\nu^* - \nu}{T} - \frac{g}{\chi RT} \right) \frac{1}{U} \frac{dU}{dz} - \frac{2}{\chi RT} \left(\frac{dU}{dz} \right)^2 \right] w = 0 \quad (5)$$

We now introduce the new dependent variable W_1 defined by —

$$w = W_1 \cdot \exp \left(\frac{g - R\nu}{2RT} z \right) \quad (6)$$

Now as the quantity $(g - R\nu)/2RT \approx (33{\cdot}8 - \nu)/2T$ per km varies little with height, we can disregard its variation with height when we differentiate equation (6) with respect to z. Equation (5) then becomes

$$\frac{\partial^2 W_1}{\partial x^2} + \frac{\partial^2 W_1}{\partial z^2} + f(z) W_1 = 0 \quad (7)$$

Where,

$$f(z) = \frac{g(\nu^* - \nu)}{U^2 T} - \frac{1}{U} \frac{d^2 U}{dz^2} + \left(\frac{\nu^* - \nu}{T} - \frac{g}{\chi RT} \right) \frac{1}{U} \frac{dU}{dz} - \frac{2}{\chi RT} \left(\frac{dU}{dz} \right)^2 - \left(\frac{g - R\nu}{2RT} \right)^2 \quad (8)$$

Equation (7) is the lee-wave equation.

3. Solution for Western Ghats

We now solve the equation (7) for the ground profile of the Western Ghats. The Western Ghats extend for about 1500 km in the N—S direction. In the west to east direction its height gradually rises to 0·8 km in a distance of 65 km and then ends in a plateau of average height 0·6 km. The average W—E vertical cross-section of the ghats is given in Fig. 1 and it can be represented by the equation —

$$\zeta_s(x) = \frac{a^2 b}{a^2 + x^2} + a' \tan^{-1} \frac{x}{a} = \int_0^\infty e^{-ak} \left(ab \cos kx + a' \frac{\sin kx}{k} \right) dk \quad (9)$$

where $\zeta_s(x)$ is the elevation of the ground surface at the level $z = -h$ with the numerical values, $h = 0{\cdot}25$ km, $a = 18$ km, $b = 0{\cdot}52$ km, and $a' = (2/\pi) \times 0{\cdot}35$ km. The axes x and z are shown in Fig. 1. In equation (9) the ridge $\zeta_1 = a^2 b/(a^2 + x^2)$ has been combined with the plateau edge $\zeta_2 = a' \tan^{-1}(x/a)$ so as to get the appropriate profile of the Western Ghats.

We now solve the lee-wave equation (7) for the ground profile given by equation(9).

For an analytical solution the function $f(z)$ defined by equation (8) is to be replaced by an analytical expression. For this Palm and Foldvik have considered only the first two terms. Scorer also, in his numerical computation, neglected the last three terms of (8) as

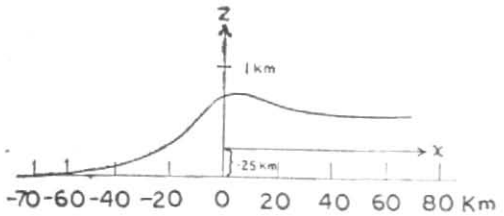

Fig. 1. Profile of Western Ghats

they were scarcely comparable with the first two. We have computed for six cases during the winter season when the wind is more or less westerly and the air is dry. We can, therefore, at this stage replace ν^* by the dry adiabatic lapse rate ν_d in which case χ becomes the ratio $c_p / c_v = 1{\cdot}4$ of specific heat at constant pressure to specific heat at constant volume. The typical numerical values taken are : $g=10^{-2}$ km/sec^2, $\chi=1{\cdot}4$, and $R=29 \times 10^{-5}$ km^2/sec/degree.

Comparison of the different terms of $f(z)$ shows that the last two terms are negligible, the second and the third terms are comparable to each other, the first term being the dominating factor. We have, accordingly, retained the first three terms. With these approximations, we have represented the observed $f(z)$ distribution below the tropospheric wind maximum by the exponential function,

$$f(z) = f_0 \, e^{-\lambda z} \tag{10}$$

where f_0 and λ are constants and this function was chosen to represent $f(z)$ in the entire atmosphere. As mentioned earlier, this will not affect the motion at low levels.

To solve the equation (7) we follow the usual procedure of assuming that the ground profile is sinusoidal, and thereafter we generalise the solution by Fourier integrals for an arbitrary mountain. For this we write

$$W_1 = W. \, e^{ikx} \tag{11}$$

Equation (7) then, with (10) and (11) reduces to the Bessel equation—

$$\eta^2 \frac{d^2W}{d\eta^2} + \eta \frac{dW}{d\eta} + \left[\eta^2 - \frac{4}{\lambda^2} k^2 \right] W = 0 \tag{12}$$

where,

$$\left.\begin{aligned} \eta &= \beta \, e^{-\lambda z/2} \\ \beta &= 2 \frac{f_0^{\frac{1}{2}}}{\lambda} \end{aligned}\right\} \tag{13}$$

The solution of the equation (12) is —

$$W = A \, J_m(\eta) + B \, Y_m(\eta)$$

$$= A \, J_m(\beta \, e^{-\lambda z/2}) + B Y_m(\beta \, e^{-\lambda z/2}) \tag{14}$$

with $m = (2/\lambda) \, k$

where $J_m(\eta)$ and $Y_m(\eta)$ are the Bessel functions of the first and second kind respectively of real order m and real argument η.

The expression for vertical velocity is thus

$$w(x, z) = \exp\left(\frac{g - R\nu}{2RT} z \right) \exp(i k x) \times$$

$$\times [A J_m(\beta \, e^{-\lambda z/2}) + B Y_m(\beta \, e^{-\lambda z/2})] \tag{15}$$

The constants A and B are to be found from the following boundary conditions —

(i) As the upper boundary condition we require that the energy of the wave remains finite at great heights. To fulfil this we use the condition —

$$w(x, z) \to 0 \text{ as } z \to \infty$$

The condition requires that in (15) $B=0$. Since the Bessel function of the second kind with real order $\to -\infty$ as its argument $\to 0$, *i.e.*, as $z \to \infty$. We thus have —

$$w(x, z) = A. \, e^{ikx} \exp\left(\frac{g - R\nu}{2RT} z \right) \times$$

$$\times J_m(\beta \, e^{-\lambda z/2}) \tag{16}$$

We use this particular solution of the wave equation for the profile (9).

(*ii*) At the lower boundary we require that the flow is tangential to the surface. For the profile (9) this condition is —

$$w(x, -h) = U(\zeta_s) \frac{\partial}{\partial x} \zeta_s(x)$$

So that the linearised lower boundary condition is —

$$w(x, -h) = U(-h) \frac{\partial}{\partial x} \int_0^\infty e^{-ak} \times$$

$$\times \left(ab \cos kx + \frac{a'}{k} \sin kx \right) dk \qquad (17)$$

The solution satisfying this condition is —

$$w(x, z) = U(-h) \frac{\exp.\left(\frac{g-R\nu}{2RT} z\right)}{\exp.\left(\frac{g-R\nu}{2RT} z\right)_{z=-h}} \cdot \frac{\partial}{\partial x}$$

$$\int_0^\infty e^{-ak} \left(ab \cos kx + a' \frac{\sin kx}{k} \right) \times$$

$$\times \frac{J_m(\beta e^{-\lambda . z/2})}{J_m(\beta e^{\lambda . h/2})} dk \qquad (18)$$

After integration, the displacement of the streamline at a level z above its original undisturbed level is —

$$\zeta(x, z) = \frac{U(-h)}{U(z)} \frac{\exp.\left(\frac{g-R\nu}{2RT} z\right)}{\exp.\left(\frac{g-R\nu}{2RT} z\right)_{z=-h}} \times$$

$$\times \int_0^\infty e^{-ak} \left(ab \cos kx + a' \frac{\sin kx}{k} \right) \times$$

$$\times \frac{J_m(\beta e^{-\lambda . z/2})}{J_m(\beta e^{\lambda . h/2})} dk \qquad (19)$$

It should be noted here that the integral in equations (18) and (19) is an improper integral as the Bessel function $J_m(\beta e^{\lambda . h/2})$ may vanish for real values of k. The improper integral is interpreted as the Cauchy Principal value of the integral. Accordingly we perform the integral in equation (19) by Cauchy's integral method along the contour shown in Fig. 2 in the complex k-plane. For this we put

$$\int_c e^{-ak} \left(ab \cos kx + a' \frac{\sin kx}{k} \right) \times$$

$$\times \frac{J_m(\beta e^{-\lambda . z/2})}{J_m(\beta e^{\lambda . h/2})} dk$$

$$= R_e \int_c e^{-ak} . e^{ikx} \left(ab - i \frac{a'}{k} \right) \times$$

$$\times \frac{J_m(\beta e^{-\lambda . z/2})}{J_m(\beta e^{\lambda . h/2})} dk, \text{ when } x > 0$$

$$\text{and} = R_e \int_c e^{-ak} . e^{-ikx} \left(ab + i \frac{a'}{k} \right) \times$$

$$\times \frac{J_m(\beta e^{-\lambda . z/2})}{J_m(\beta e^{\lambda . h/2})} dk, \text{ when } x < 0 \qquad (20)$$

where c is the path of integration and R_e is the real part and $i = (-1)^{\frac{1}{2}}$. It can be seen that the order of Bessel function $m = (\lambda/2)k$ can assume complex values in the process of integration. The zeros of $J_m(\beta e^{\lambda . h/2})$ regarded as a function of m, are real for positive values of the argument $\beta e^{\lambda . h/2}$. The integrand in (20) has, therefore, poles for only real values of m, *i.e.*, of k, so that the path of integration has indentations along the real axis of the complex k-plane. It is the roots of $J_m(\beta e^{\lambda . h/2}) = 0$ that determine lee-waves. The integral along the circular arc tends to zero as its radius R tends to infinity.

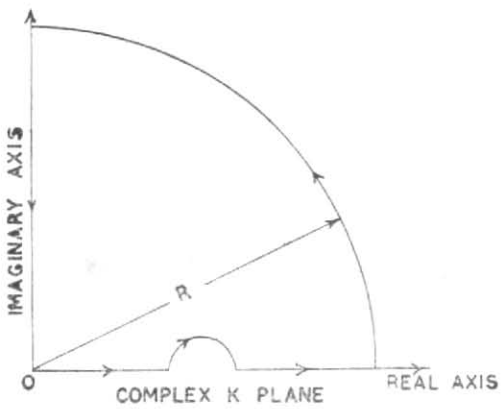

Fig. 2. Paths for contour integration

It may be mentioned here that the solution is not unique when the motion is assumed stationary and free waves exist. Such a difficulty does not arise when the problem is considered as an initial value problem. Different methods have been devised to render the solution unique, when the motion is assumed stationary. Rayleigh (1883) rendered the problem unique by introducing the small frictional forces proportional to velocity. In the final solution these forces were put equal to zero. Kelvin (1886) devised another method to make the problem determinate from the physical reasoning that all waves should vanish at large distance upstream from the region of disturbance. His method, accordingly, consists of adding free waves with such amplitudes and wavelengths that there will be no waves extending to infinity upstream. We have here made use of this method.

Performing the integrations as above and making the radii of the indentations tend to zero and the radius of the circular arc R tend to infinity and applying Kelvin's monotony condition we find that the solution of $\zeta\ (x, z)$ can be adequately divided into two parts ζ_p and ζ_r as follows—

$$\zeta\ (x, z) = \zeta_p + \zeta_r \tag{21}$$

where,

$$\left.\begin{aligned}\zeta_p = {} & \frac{U\ (-h)}{U\ (z)} \cdot \frac{\exp.\left(\frac{g-R\nu}{2RT}\, z\right)}{\exp.\left(\frac{g-R\nu}{2\,RT}\, z\right)_{z=-h}} \times \\ & \times I \int_0^{\infty} e^{-ik} \cdot\ e^{-kx}\left(-ab + \frac{a'}{k}\right) \times \\ & \times \frac{J_{im}\ (\beta e^{-\lambda . z/2})}{J_{im}\ (\beta\, e^{\lambda . h/2})}\ dk \\ \zeta_r = {} & \frac{U\ (-h)}{U(z)} \cdot \frac{\exp.\left(\frac{g-R\nu}{2\,RT}\, z\right)}{\exp.\left(\frac{g-R\nu}{2\,RT}\, z\right)_{z=-h}} \times \\ & \times 2\,\pi \sum_{n=1}^{N} e^{-akn}\left(-ab \sin k_n\, x + \right. \\ & \left. + a'\ \frac{\cos k_n\, x}{k_n}\right) \times \frac{J_{m_n}\ (\beta\, e^{-\lambda . z/2})}{\frac{d}{dk}\, J_{m_n}(\beta\, e^{\lambda . h/2})}\end{aligned}\right\} \begin{matrix}(21a)\\ x<0\end{matrix}$$

and

$$\left.\begin{aligned}\zeta_p = {} & \frac{U\ (-h)}{U(z)} \cdot \frac{\exp.\left(\frac{g-R\nu}{2\,RT}\, z\right)}{\exp.\left(\frac{g-R\nu}{2\,RT}\, z\right)_{z=-h}} \times \\ & \times I \int_0^{\infty} e^{-ik} \cdot\ e^{kx}\left(-ab - \frac{a'}{k}\right) \times \\ & \times \frac{J_{im}\ (\beta\, e^{-\lambda . z/2})}{J_{im}\ (\beta\, e^{\lambda . h/2})}\ dk \\ \zeta_r = {} & 0\end{aligned}\right\} \begin{matrix}(21b)\\ x<0\end{matrix}$$

where I means the imaginary part.

k_n is given by $m_n = (\lambda/2)\, k_n$

m_n's being the roots of $J_m(\beta e^{\lambda \cdot h/2}) = 0$ (22)

Similarly, for the vertical velocity we have

$$w(x, z) = w_p + w_r \tag{23}$$

where,

$$\left.\begin{aligned} w_p = U(-h). \frac{\exp.\left(\frac{g-R\nu}{2RT} z\right)}{\exp.\left(\frac{g-R\nu}{2RT} z\right)_{z=-h}} \times \\ \times I \int_0^\infty e^{-iak} e^{-kx} (abk - a') \times \\ \times \frac{J_{im}(\beta e^{-\lambda . z/2})}{J_{im}(\beta e^{\lambda . h/2})}\, dk \\ w_r = -U(-h). \frac{\exp.\left(\frac{g-R\nu}{2RT} z\right)}{\exp.\left(\frac{g-R\nu}{2RT} z\right)_{z=-h}} \times \\ \times 2\pi \sum_{n=1}^{N} e^{-ak_n} (a\, b\, k_n \cos k_n x + \\ + a' \sin k_n x) \frac{J_{m_n}((\beta e^{-\lambda . z/2})}{\frac{d}{dk} J_{m_n}(\beta e^{\lambda . h/2})} \end{aligned}\right\} \begin{matrix} (23a) \\ x>0 \end{matrix}$$

and

$$\left.\begin{aligned} w_p = U(-h). \frac{\exp.\left(\frac{g-R\nu}{2RT} z\right)}{\exp.\left(\frac{g-R\nu}{2RT} z\right)_{z=-h}} \times \\ \times I \int_0^\infty e^{-iak} \cdot e^{kx} (-a\, b\, k - a') \times \\ \times \frac{J_{im}(\beta e^{-\lambda . z/2})}{J_{im}(\beta e^{\lambda . h/2})}\, dk \\ w_r = 0 \end{aligned}\right\} \begin{matrix} (23b) \\ x<0 \end{matrix}$$

Equations (21) and (23) are the final solutions giving waves downstream only.

For ease of computation we put ζ_r and w_r in the following simplified forms —

$$\zeta_r = -\frac{U(-h)}{U(z)} \cdot \frac{\exp.\left(\frac{g-R\nu}{2RT} z\right)}{\exp.\left(\frac{g-R\nu}{2RT} z\right)_{z=-h}} \times$$

$$\times 2\pi \sum_{n=1}^{N} e^{-akn} A(k_n). \frac{J_{m_n}(\beta . e^{-\lambda . z/2})}{\frac{d}{dk} J_{m_n}(\beta . e^{\lambda . h/2})} \times$$

$$\times \sin(k_n x + \alpha_n); \qquad x>0 \tag{24a}$$

$$w_r = -U(-h). \frac{\exp.\left(\frac{g-R\nu}{2RT} z\right)}{\exp.\left(\frac{g-R\nu}{2RT} z\right)_{z=-h}} \times$$

$$\times 2\pi \sum_{n=1}^{N} e^{-akn} A(k_n). k_n. \frac{J_{m_n}(\beta . e^{-\lambda . z/2})}{\frac{d}{dk} J_{m_n}(\beta . e^{\lambda . h/2})} \times$$

$$\times \cos(k_n x + \alpha_n); \qquad x>0 \tag{24b}$$

$$\left.\begin{aligned} \text{where, } A(k) = \left(a^2 b^2 + \frac{a'^2}{k^2}\right)^{\frac{1}{2}} \\ \alpha = \tan^{-1}\left(-\frac{a'}{kab}\right) \end{aligned}\right\} \tag{24c}$$

In (21) and (23) ζ_r and w_r consist of a sum of harmonic lee waves and constitute the real wave motion. It is seen that $\zeta_r = 0$ at $z = -h$ (ground) and discontinuous at $x = 0$. Therefore ζ_p satisfies the boundary condition at $z = -h$ and has the same kind of singularity as that of ζ_r for $x = 0$ in order to make the complete solution analytic. It is thus clear that ζ_p or w_p is important near the mountain and this term dies away very rapidly at a rate $e^{-2\pi}$ per wavelength as $|x|$ increases. In the

TABLE 1

Case No.	Date (time)	$f(0)$ km^{-2}	λ km^{-1}	$\beta e^{\lambda.h/2}$	Wavelength L
1	5 March 1962 (00 Z)	9·60	0·50	13·3	26·2 7·8 4·4 2·8
2	6 December 1960 (12 Z)	5·21	0·34	14·0	25·1 10·0 5·9 3·9
3	21 January 1959 (12 Z)	8·15	0·45	13·4	26·2 8·3 4·9 3·1
4	4 January 1959 (12 Z)	6·79	0·44	12·5	62·8 10·8 5·6 3·5
5	14 December 1960 (00 Z)	17·11	0·47	18·7	69·7 10·6 5·6 3·6 2·6 1·9
6	26 December 1960 (12 Z)	11·96	0·46	15·5	78·5 11·2 5·7 3·6 2·5

present paper we are primarily interested in the wave set up by the mountain and have, therefore, computed only ζ_r and w_r. The results will not, therefore, be strictly valid near the mountain.

3.1. *Determination of wave length* — We have approximated the observed $f(z)$ profile from 1 km (to avoid friction layer) to the tropospheric wind maximum by an exponential function. According to Palm and Foldvik (1960) this representation will give a good approximation of the solution obtained when the real distribution of $f(z)$ at higher levels is considered provided the following conditions are satisfied —

(*i*) $f_2 > 2{\cdot}5\, f_1$ where f_2 and f_1 are the maximum and minimum values of $f(z)$. This condition is satisfied for all the cases we have examined.

(*ii*) Exclusion of wave numbers for which $k^2 < f_1$ from the solution of the equation $J_m(\beta.e^{\lambda.h/2}) = 0$. In other words, wavelengths greater than the critical wavelength L_s determined by the minimum value of $f(z)$ should not be considered.

However, Foldvik (1962) has shown that the one-layer model gives good approximation even in the region $k^2 < f_1$, *i.e.*, even for wavelengths greater than the critical wavelength. In the cases studied by him waves have actually been observed of lengths near to the computed long waves for which $k^2 < f_1$. This is also in consistence with the results of investigation of Eliassen and Palm (1961) in the reflection of wave energy in atmosphere. They found that in the region $k^2 > f_1$ almost all the energy was

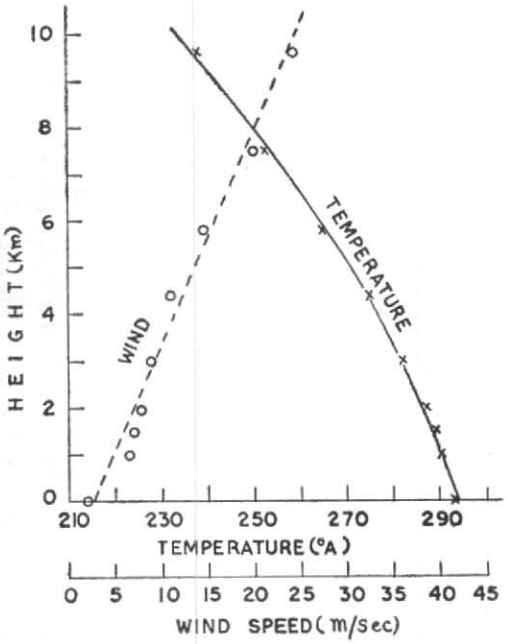

Fig. 3 (a). Wind and temperature of Santacruz of 5 March 1962 (00Z)

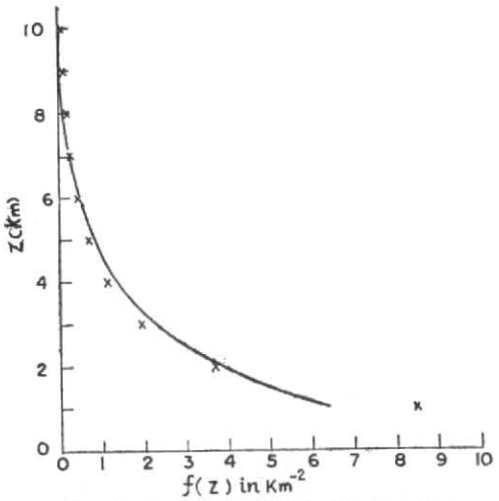

Fig. 3(b). $f(z)$ profile of 5 March 1962 (00Z)

reflected from above and that even in the region $k^2 < f_1$ a considerable amount of energy was reflected. Thus for the 3-layer model described by Palm and Foldvik (1960) reflected part of wave energy is 82 per cent for $k^2 = f_1 = 0{\cdot}05/\text{km}^2$ (L_s=26 km) and 65 per cent when k=0·1/km (L=63 km). The solution for which $k^2 < f_1$ should, therefore, not be rejected but be considered as an approximation to the correct wavelength. Accordingly, we have taken all the solutions of the equation (22) irrespective of whether $k^2 >$ or $< f_1$. It is seen that in all the cases except one, the computed longer waves are greater than their corresponding critical wavelengths and it is found that the Western Ghats being very broad, it is only these waves that give recognisable displacement and vertical velocity and the shorter waves do not practically give any effect.

3.2. *Numerical computation* — For selecting cases for numerical study of mountain waves over Western Ghats one is handicapped with having no observation on mountain wave phenomenon. Accordingly, from an examination of wind and temperature data we have taken few cases that are normally believed to be favourable for the occurrence of mountain-waves. For the undisturbed wind and temperature we have taken the data of Santacruz which is a sea level station on the wind-ward side of the Western Ghats at

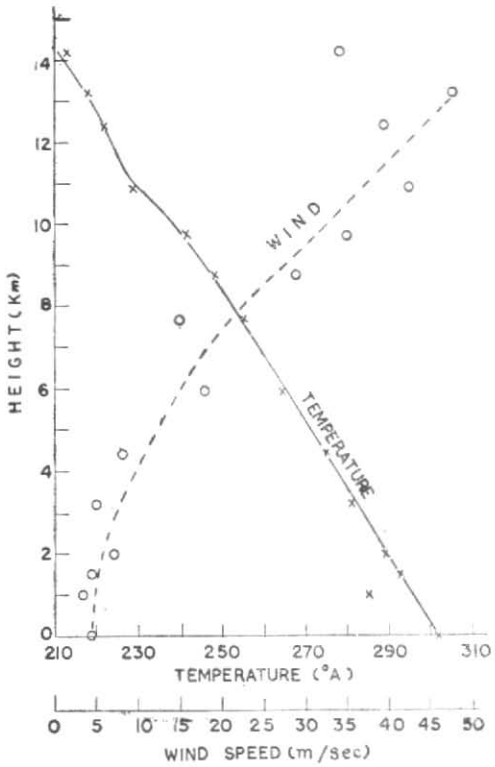

Fig. 4(a). Wind and temperature of Santacruz of 6 December 1960 (12Z)

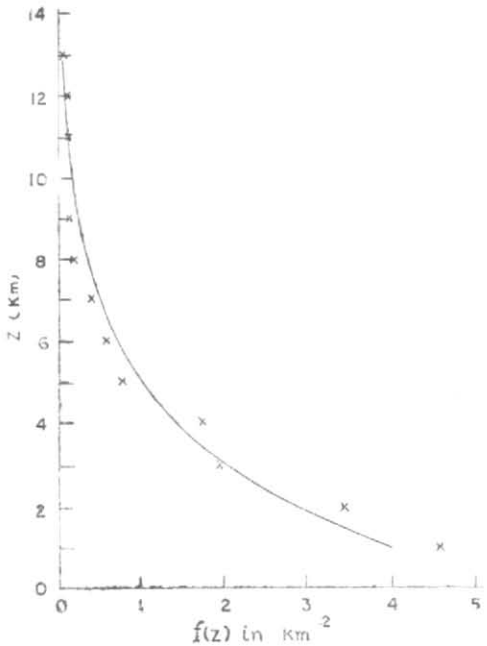

Fig. 4 (b). $f(z)$ profile of 6 December 1960 (00Z)

a distance of 64 km from the peak. The wind and temperature distribution and the corresponding $f(z)$ distribution are given in Figs. 3—8. The actual distribution of wind and temperature are represented by circles and crosses respectively and the corresponding smoothed distributions by dashed lines and continuous lines respectively. The actual distribution of $f(z)$ is shown by crosses and continuous line shows exponential approximation. The parameters f_0, λ, $\beta e^{\lambda h/2}$ and computed wave length L for the different cases are shown in Table 1. We now discuss the different cases.

Case No. I — 3 March 1962 (00 GMT)

The wind and temperature distributions are given in Fig. 3(a) and the corresponding $f(z)$ profile in Fig. 3 (b). The wind increases linearly from 2·7 m/sec to 25 m/sec at 10-km level with an average wind shear of 2·2 m/sec/km. The atmosphere is stable throughout. But the stability is more at low levels than at higher levels. The lapse rate increases from 3·8°C/km at 1-km level to 9·1°C/km at 10 km. The exponential representation of $f(z)$ is good except at 1-km level where the difference is of the order of 2·5/km^2. The lee-wave equation

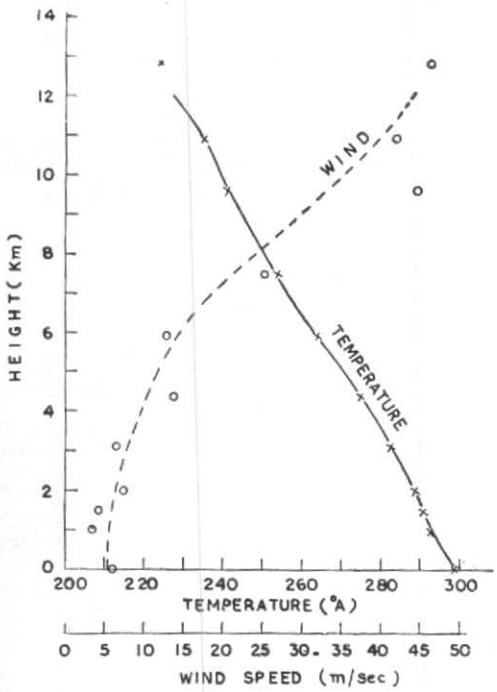

Fig. 5 (a). Wind and temperature of Santacruz of 21 January 1959 (12Z)

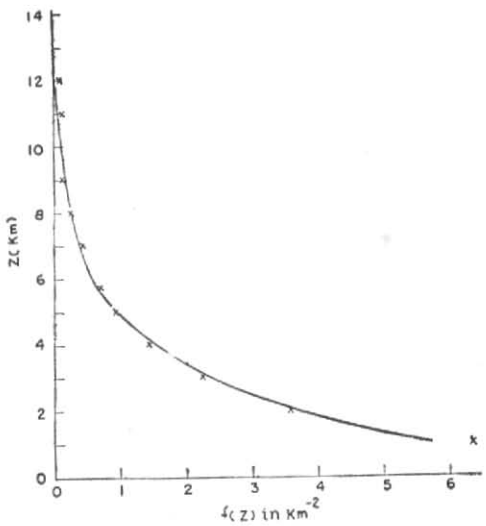

Fig. 5 (b). $f(z)$ profile of 21 January 1959 (12Z)

gives four roots, the corresponding wavelengths being 26·2, 7·8, 4·4 and 2·8 km. The longest wavelength is the only important wave for the Western Ghats. The other short waves do not contribute to the wave motion. The variation of amplitude of streamline displacement with height for this wave is represented in Fig. 9 (a) and the variation of vertical velocity with height is shown in Fig. 10 (a). We have represented these variations up to 8 km for, the solution as mentioned earlier, may not be strictly valid above this level. It is seen that there are three reversal of phases below 8 km indicating the presence of at least three cellular motions below the motion of external type above. The maximum amplitude is 100 m and the maximum vertical velocity is 0·4 m/sec at a height of 8 km. Values above 10 km could not be computed because of lack of data.

Case No. II—6 December 1960 (12 GMT) —Figs. 4a, 4b

The wind speed increases from 5 m/sec to 47 m/sec at 14 km. The shear increases with height and above 7 km it is of the order of 4 to 5 m/sec/km. Lapse rate although is of the order of 6·25°C/km. The exponential approximation of $f(z)$ is good above 2 km. The lee-wave equation gives four roots, the corresponding wavelengths being 25·1, 10·0, 5·9 and 3·9 km. The longest wave length is the only important

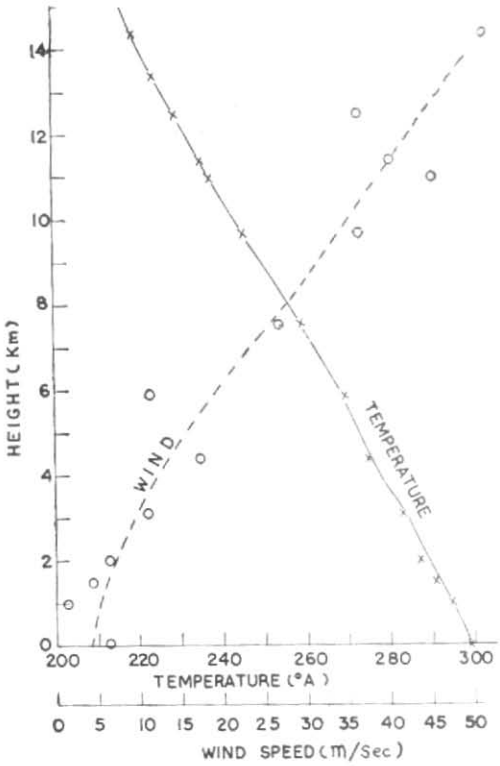

Fig. 6(a). Wind and temperature of Santacruz of 4 January 1959 (12Z)

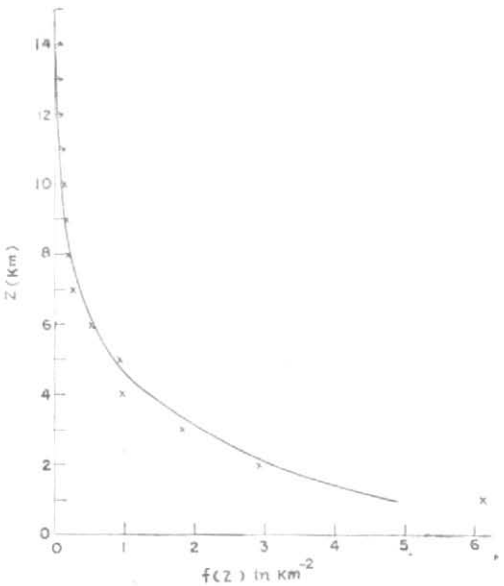

Fig. 6(b). $f(z)$ profile of 4 January 1959 (12Z)

one in our case. There are three reversal of phases within 8 km. (Figs. 9a, 10a). It will be seen from these figures that within 8 km the maximum amplitude is 50 m and maximum vertical velocity is 0·2 m/sec. The vertical velocity, however, is maximum at 12 km and the value is 0·4 m/sec.

Case No. III — 21 January 1959 (12 GMT) — Figs. 5a, 5b

The wind speed increases from 5 m/sec to 44 m/sec at 12 km. Below 6 km the wind shear is less than 3 m/sec/km. The shear increases gradually and is of the order of 5 to 6 m/sec/km in the levels 8—10 km. The temperature lapse rate above 2 km is about 6°C/km and below 2 km it varies from 4 to 5°C/km. The exponential representation of $f(z)$ is good except at 1 km. The lee-wave equation gives four roots, the corresponding wavelengths being 26·2, 8·3, 4·9 and 3·1 km. The longest wavelength only is important. From Figs. 9(a) and 10(a) it will be seen that the maximum amplitude and vertical velocity within 8 km are 120 m and 0·5 m/sec respectively. The vertical velocity within 12 km is maximum at 10 km, the value being 0·6 m/sec.

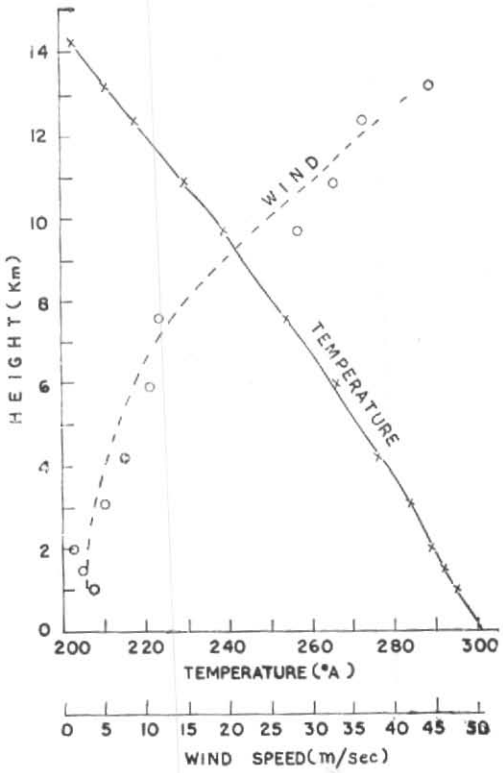

Fig. 7(a). Wind and temperature of Santacruz of 14 December 1960 (00Z)

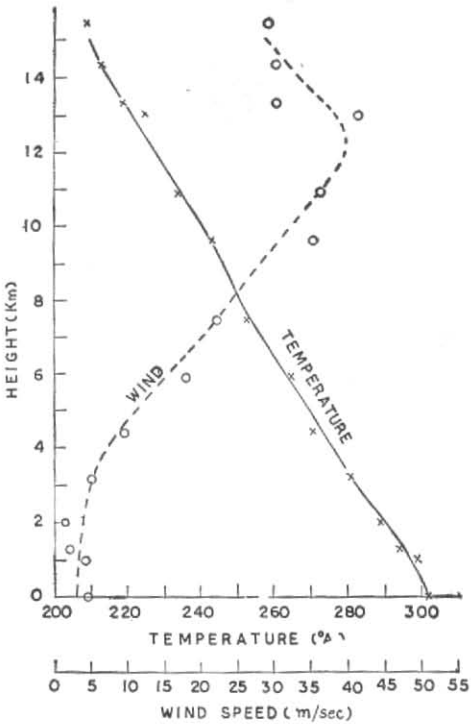

Fig. 8 (a). Wind and temperature of Santacruz of 26 December 1960 (12Z)

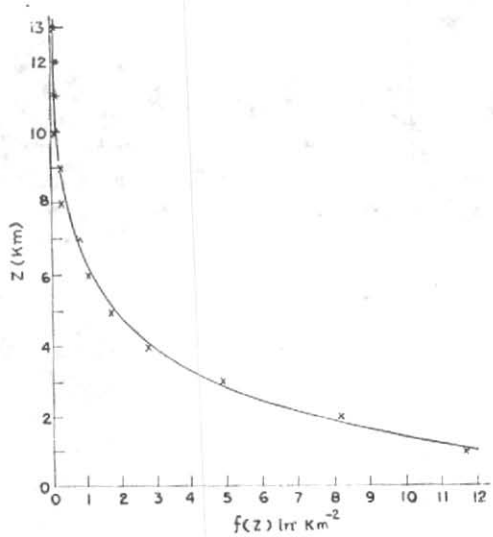

Fig. 7(b). $f(z)$ profile of 14 December 1960 (00Z)

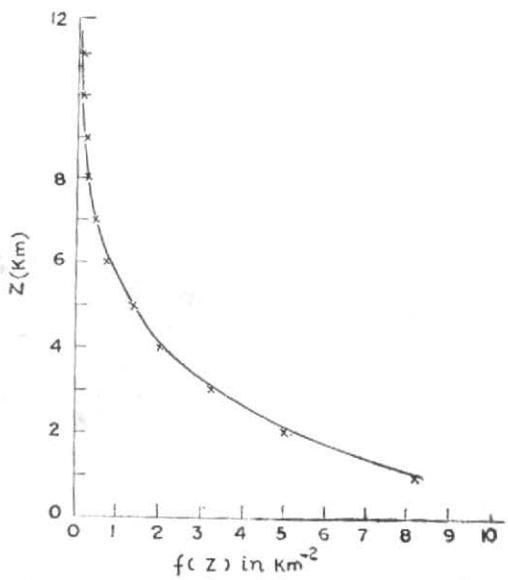

Fig. 8(b). $f(z)$ profile of 26 December 1960 (12Z)

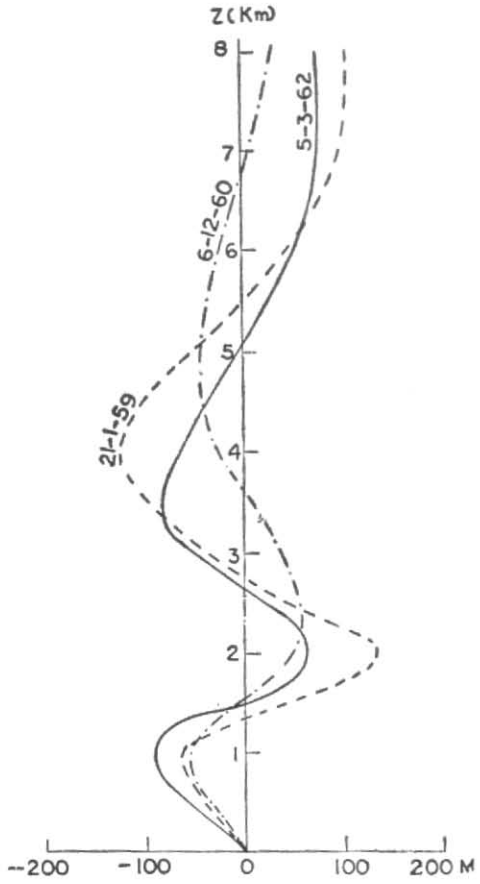

Fig. 9(a)

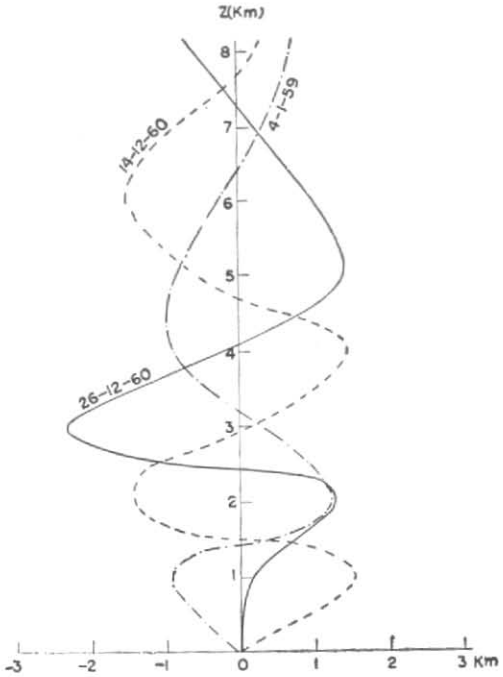

Fig. 9(b)

Figs. 9 (a) and 9 (b). Variation of amplitude [for sin $(kx+\alpha)=1$] with height

Case No. IV — 4 January 1959 (12 GMT) —Figs. 6a, 6b

The wind speed increases from 4·1 m/sec to 49 m/sec at 14 km. The wind shear above 3 km varies from 3 to 4 m/sec/km. The lapse rate is of the order of 5°C/km up to 6 km above which it is of the order of 6°C/km. The exponential representation of $f(z)$ is fairly good except at 1 km. The lee-wave equation gives four solutions, the corresponding wavelengths being 62·8, 10·8, 5·6 and 3·5 km. The longest wavelength only is important. It is seen from Figs. 9(b) and 10(b) that within 8 km there are three reversal of phases indicating at least three cellular motions below the motion of external type above. The amplitude of the displacement of streamline is considerably more. The maximum displacement is 1200 m at 2 km (Fig. 9b) and maximum vertical velocity is 1·9 m/sec at 8 km (Fig. 10b). The velocity increases still higher up and becomes maximum at 15 km where the value is 4·8 m/sec.

Case No. V — 14 December 1960 (00 GMT) — Figs. 7a, 7b

The wind speed increases from 2·5 m/sec to 45 m/sec at 13 km. Upto 7 km the wind

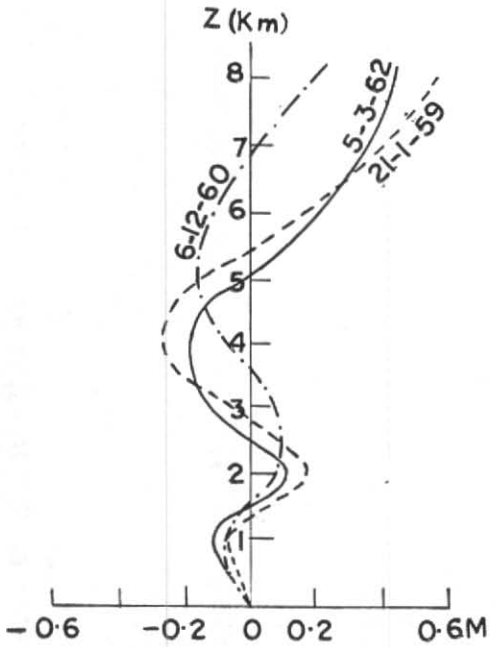

Fig. 10(a)

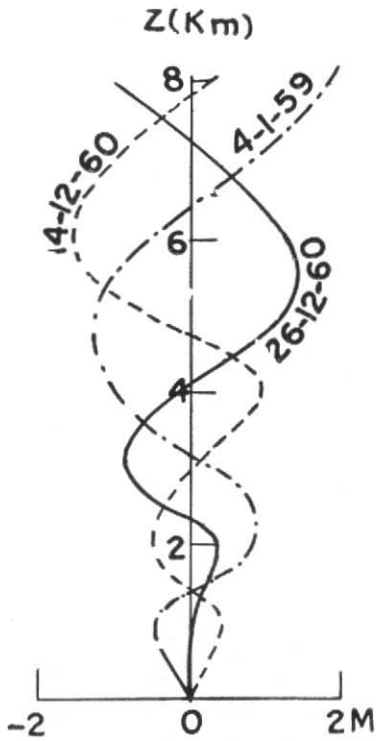

Fig. 10(b)

Figs. 10 (a) and 10 (b). Variation of vertical velocity [for cos $(kx+\alpha)=1$] with height

shear is of the order of 2 m/sec/km. Above 8 km the shear varies from 5 to 6 m/sec/km. The lapse rate is of the order of 7°C/km. The exponential approximation of $f(z)$ is very good throughout. The lee-wave equation gives six-roots, the corresponding wavelengths being 69·7, 10.6, 5·6, 3·6, 2·6 and 1·9 km. The longest wave only is important. Figs. 9(b), 10(b) show that there are four reversal of phase within 8 km. Within 8 km the maximum displacement is 600 m at 6 km and the maximum vertical velocity is 1·6 m/sec at 6 km. At higher levels the velocity is more and maximum velocity is 5·2 m/sec at 14 km above which data are not available.

Case No. VI — 26 December 1960 (12 GMT) — Figs. 8a, 8b

The wind speed increases from 3 m/sec to 40 m/sec at 12 km. The wind decreases thereafter to 30 m/sec at 15 km which we have not considered for computation of $f(z)$. This will not affect the solution, as mentioned earlier. The shear is small below 5 km but in the layer 5-10 km the shear is of the order of 4 to 5 m/sec/km. Temperature lapse rate is about 7° C/km at low levels. In the layer 5-9 km, the lapse rate is about 5°C/km. The exponential representation of $f(z)$ is very good. The lee-wave equation gives five roots, the corresponding wavelengths being 78·5, 11·2, 5·7, 3·6 and 2·5 km. The

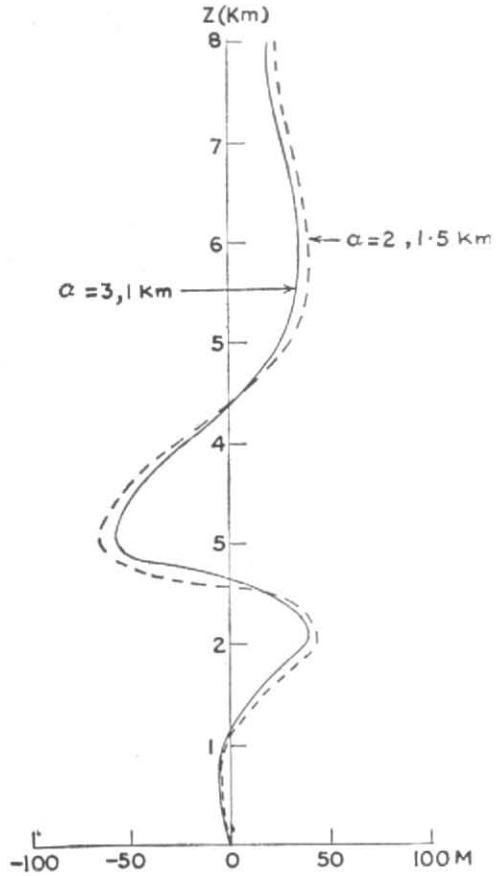

Fig. 11(a). Variation of amplitude (for sin $kx=1$) with height for second wave ($L_2=11{\cdot}2$ km) on 26 December 1960 for small mountain. $\zeta=a^2b/(a^2+x^2)$ with $b=0{\cdot}1$ km and a having values 1, 1·5, 2 and 3 km

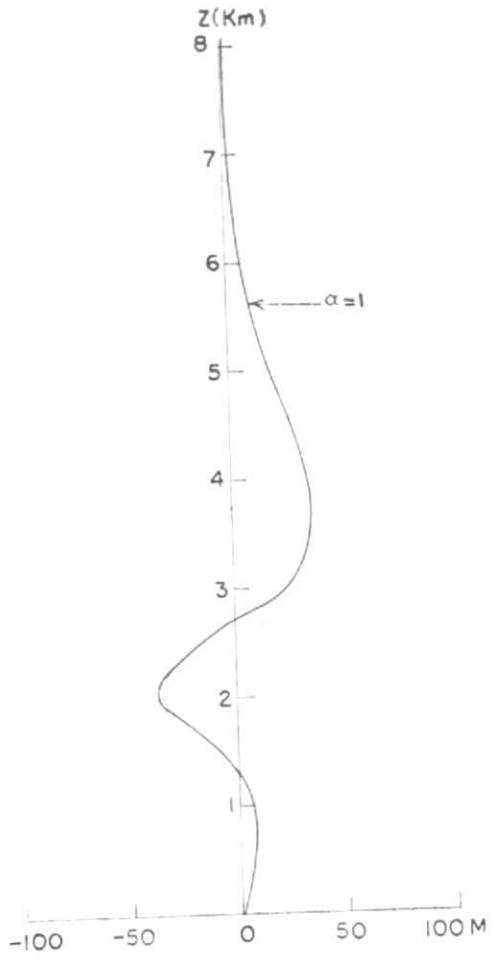

Fig. 11(b). Variation of amplitude (for sin $kx=1$) with height for third wave ($L_3=5{\cdot}7$ km) on 26 December 1960 for small mountain. $\zeta=a^2b/(a^2+x^2)$ with $b=0{\cdot}1$ km and $a=1$ km

longest wavelength only is important. Within 8 km, there are three reversal of phases, the maximum displacement is 2200 m at 3 km and the maximum vertical velocity is 1·3 m/sec at 6 km (Figs. 9b, 10b). The velocity is more at higher levels and the maximum value 5·7 m/sec occurs at 15 km above which value cannot be computed because of lack of data. The streamlines at the levels 2, 4, 6 and 8 km for the longest wave are shown in Fig. 13(a). The streamlines consisting of only one wave are sinusoidal. The reversals of phases are distinct from the diagram. As the term which is important near the mountain has not been considered, the streamline pattern as shown in this figure will not strictly be valid in the vicinity of the mountain.

3.3. *The shorter waves* — We have mentioned earlier that the shorter waves of lengths below 20 km are not important. This is, perhaps, due to the fact that Western Ghats mountain is very broad. In order to

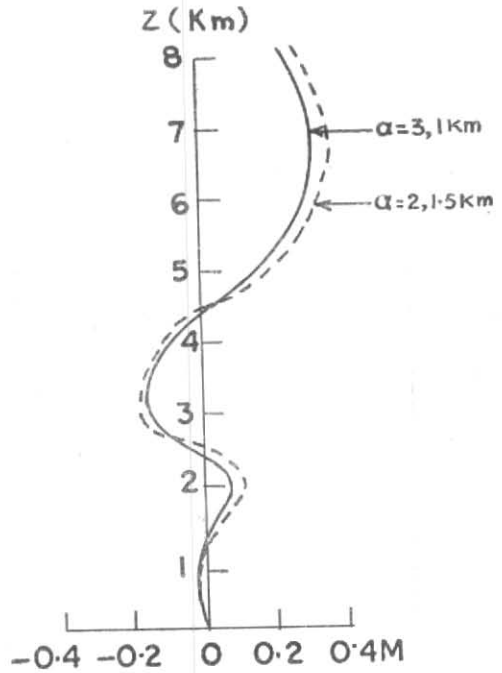

Fig. 12(a). Variation of vertical velocity (for cos $kx=1$) with height for the second wave ($L_2=11\cdot2$ km) on 26 December 1960 for a small mountain. $\zeta=a^2b/(a^2+x^2)$ with $b=0\cdot1$ km and a having values 1, 1·5, 2 and 3 km

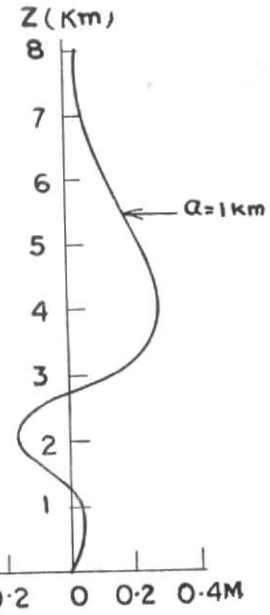

Fig. 12(b). Variation of vertical velocity (for cos $kx=1$) with height for the third wave ($L_3=5\cdot7$ km) on 26 December 1960 for a small mountain. $\zeta=a^2b/(a^2+x^2)$ with $b=0\cdot1$ and $a=1$ km

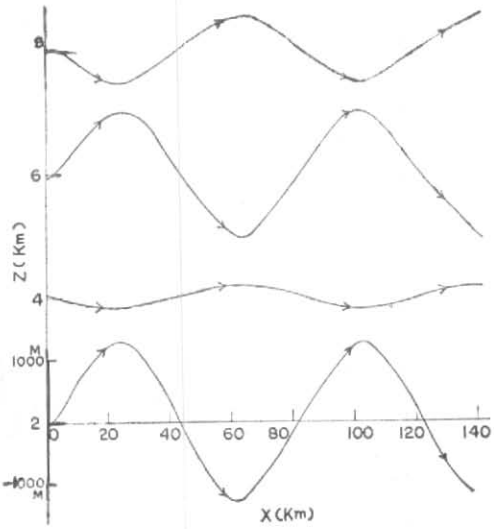

Fig. 13(a). Streamlines at levels 2, 4, 6 and 8 km for the longest wave $L_1=78\cdot5$ km on 26 December 1960 (12Z)

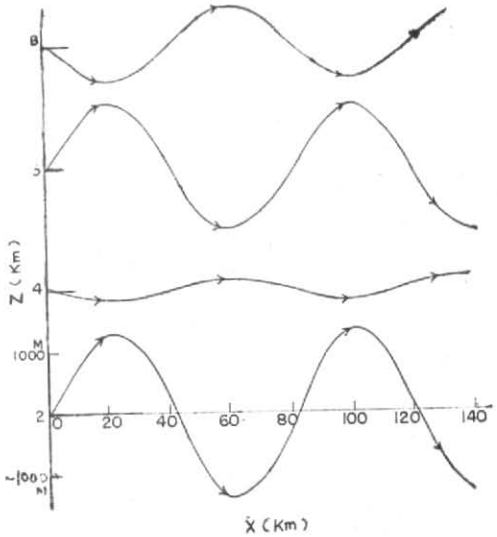

Fig. 13(b). Streamlines at levels 2, 4, 6 and 8 km for the two waves $L_1=78\cdot5$ km and $L_2=11\cdot2$ km on 26 December 1960 (12Z) for the superposed ridge. $\zeta=a^2b/(a^2+x^2)$ with $a=3$ km and $b=0\cdot1$ km on the Western Ghats

examine the point in detail we consider the second and third waves of 26 December 1960 (Case No. VI). These waves are of lengths L_2=11·2 km and L_3=5·7 km respectively. For these waves we have computed the amplitudes and vertical velocities for some narrow symmetrical ridges $\zeta = (a^2b)/(a^2 + x^2)$, ($b$ is the height of the ridge and a is the half width). For wave length 11·2 km we have computed for four case, *viz.*, a=3·2, 1·5 and 1 km and b=0·1 km and for wave length 5·7 km we have computed for one case, *viz.*, a = 1 km, b=0·1 km. The changes of amplitudes and vertical velocities with height are given in Figs. 11(a), 11(b), 12(a), 12(b). It will be seen from these diagrams that these amplitudes and vertical velocities are not negligible. For the wavelength 11·2 km, there are three reversal of phases (Figs. 11a, 12a) within 8 km indicating at least three cellular motions below the motion of external type above. The maximum amplitude for this case is 65 m at 3 km and the maximum vertical velocity is 0·36 m/sec at 7 km. For the third wave of length 5·7 km there are two reversal of phases (Figs. 11b, 12b) within 8 km. The maximum amplitude is 37 m at 2 km and the maximum vertical velocity is 0·28 m/sec at 4 km. It is thus clear that the shorter waves which were found unimportant for a broad mountain like Western Ghats give appreciable displacements of streamlines for narrow mountains.

In order to see how the streamlines will look like when the first two waves (L_1=78·5 km and L_2=11·2 km) are superposed we have superposed the narrow mountain $\zeta = (a^2b)/(a^2 + x^2)$, ($a$=3 km, b=0·1 km) at the origin on the Western Ghats profile. By this superposition the Western Ghats is slightly changed. The peak which was at a distance of 4 km from the origin now shifts to the origin and the maximum height increases from 0·8 km to 0·87 km and the rest of the profile is practically not changed. The superposed streamline field (for the waves only) for the new profile is given in Fig. 13(b). The contribution of the longest wave L_1=78·5 km for the narrow ridge $\zeta = (a^2 b)/(a^2+x^2)$ is about one-tenth of the contribution for the original Western Ghats profile and the contribution of the second wave L_2=11·2 km due to the ridge $\zeta=(a^2 b)/(a^2+x^2)$ is still less. A comparison of this Fig. 13(b) with Fig. 13(a) will show that the regular sinusoidal pattern of the streamline field is only slightly changed due to this superposition.

4. Discussion of the results

We have seen that only the longer waves are important for the Western Ghats. So our discussion will be only for these waves. As will be seen from the Figs. 3—8 that the cases studied are not such as to enable one to discuss the effect of variation of temperature distribution and of the wind profile separately. For the comparative discussion, we group together cases 1—3 in group A and cases 4—6 in group B. Cases 1—3 in Group A have wavelengths 26·2, 25·1 and 26·2 km respectively.

Comparison of case 1 and case 3 shows that up to 7 km both wind speed and stability are slightly more in case 1 and that above 7 km they are less in case 1. It appears that more wind speed and stability below and less stability and less wind speed above are so adjusted that the $f(z)$ profile in two cases are same giving same wavelength.

Comparison of cases 2 and 3 shows that wind speed and wind shear is practically same throughout for both. The temperature distribution is also more or less similar with the result that the wavelengths are near to each other. They differ by only 1·1 km, which is very small considering the approximations made in computation.

Cases 4—6 in group B have the wavelengths 62·8, 69·8 and 78·5 km respectively.

Comparison of cases 4 and 5 shows that in case 4, wind speed is more throughout. The stability is same in both the cases up to 4 km above which stability is more in case 4.

It seems more wind speed and more stability in case 4 were responsible for making the wavelength shorter by 6·9 km than case 5.

Comparison of case 4 and case 6 also leads to the same inference.

Comparison of cases 5 and 6 is not easy. The wind speed was same up to 3 km. The wind speed was more up to 10 km in case 6. But the wind shear is considerably more in case 5 from 7 km above. The stability is more at least up to 8 km in case 5. Perhaps in this case the stability and the wind shear rather than the wind speed played the dominant role in determining the wavelengths.

It is difficult to compare the groups A and B. But in general it appears both wind speed and stability are more in group A than in group B.

5. Conclusions

We can draw the following conclusions from the present study —

(*i*) The air stream of winter season has the favourable stable stratification for producing mountain waves over the Western Ghats.

(*ii*) The Western Ghats being very broad do not give appreciable amplitude for shorter waves. Only the waves of lengths 25 km and more are important.

(*iii*) For these waves three or more cellular motions exist below the motion of external type above.

(*iv*) Amplitude of waves increases with wavelength. For waves of length 26 km the maximum amplitude within 8 km is 120 m, whereas the amplitude ranges from 1200 to 2200 m for waves of lengths 62·8 to 78·5 km.

(*v*) In the range of wavelengths 25—78·5 km, the maximum vertical velocity increases with wavelength. The maximum vertical velocity for a wave of length 26·2 km is 0·6 m/sec, whereas for waves of lengths 62·8 to 78·5 km, the vertical velocity varies from 4·8 to 5·6 m/sec.

(*vi*) The vertical velocity has maximum at a height which appears to increase with wavelength.

It must, however, be recognised that the one-layer model from which we have made all the computations is not strictly valid at higher levels. From which level the model will not be valid is difficult to say.

6. Acknowledgement

The author is very much thankful to Dr. P.R. Pisharoty, Director of the Institute of Tropical Meteorology for his keen interest and kind encouragement in this investigation. The author is also indebted to Prof. R. S. Scorer of Imperial College of Science and Technology, London, for suggesting equation (9) for the Western Ghats profile and for useful suggestions in preparation of the paper.

REFERENCES

Corby, G. A. and Sawyer, J. S.	1958	*Quart. J. R. met. Soc.*, **84**, p. 25.
Eliassen, A. and Palm, E.	1961	*Geof. Publ.*, **22**, 3, Oslo.
Döös, Bo. R.	1958	Tech. Report No. 13 Contract No. Nour 6000(00). Florida State University, Florida.
	1961	*Tellus*, **13**, p. 305.
	1962	*Ibid.*, **14**, p. 301.
Foldvik, A.	1962	*Quart. J.R. met. Soc.*, **88**, p. 271.

REFERENCES (contd)

Foldvik A. and Palm, E.	1957	Inst. Weather and Climate Research. Oslo Report No. 7.
	1959	*Ibid.*, Oslo Report No. 4.
	1960	*Geof. Publ.*, **21**, **6**, Oslo.
Kelvin, Lord	1886	*Phil. Mag.*, **5**, 22, pp. 353, 445, 517.
Lyra, G.	1943	*Z. Angew Math. Mech.*, 26, p. 1.
Palm, E.	1958	*Geof. Publ.*, **20**, 2, Oslo.
Queney	1947	*Misc. Rep.*, 23, Dep. Met. Univ. Chicago.
Queney, P. *et al.*	1960	*W.M.O. Tech. Note*, 34.
Rayleigh, Lord	1883	*Proc. Lond. math. Soc.*, 15, p. 69.
Sawyer, J. S.	1960	*Quart. J. R. met. Soc.*, **86**, p. 326.
Scorer, R. S.	1949	*Ibid.*, **75**, p. 41.
	1953	*Ibid.*, **79**, p. 70.